Environmental Science and Pollution Research (2023) 30:71103–71119
https://doi.org/10.1007/s11356-023-27104-z

RESEARCH ARTICLE

Big data–driven carbon emission traceability list and characteristics of ships in maritime transportation—a case study of Tianjin Port

Peng Wang[1,2] · Qinyou Hu[1] · Wenxin Xie[3] · Lin Wu[2] · Fei Wang[2] · Qiang Mei[1,4]

Received: 31 January 2023 / Accepted: 14 April 2023 / Published online: 9 May 2023

Abstract

As Chi na's shipping industry continues to develop, ship emissions have become a significant source of pollutants. Consequently, it has become imperative to comprehend accurately the nature and attributes of ship pollutant emissions and understand their causation and effect as a crucial aspect of pollution control and legislation. This paper employs high-precision automatic identification system (AIS) dynamic and static data, along with pollutant emission parameters, to estimate the pollutant emissions from a ship's main engine, auxiliary engine, and boiler using a dynamic approach. Additionally, the study considers the sailing state and trajectory of the vessel and analyzes the characteristics of ship carbon emissions. Taking Tianjin Port as an example, this study conducts a multi-dimensional analysis of pollutant emissions to gain insight into the causation and effect of pollutants based on the collected big AIS data. The results show that the pollutant emissions in this region are mainly concentrated in the vicinity of Tianjin Port land port area, Dagusha Channel, and the Main Shipping Channel of Tianjin Xingang Fairway. Carbon emissions peak in September and are lower in June and December. Through accurate analysis of pollutant emission sources and emission characteristics in the region, this paper establishes the regular relationship between pollutant emissions and possible influencing factors and provides data support for China to formulate accurate pollutant emission reduction policies and regulate ship construction technology and carbon trading.

Keywords Marine environment protection · Ship pollutants · Automatic identification system (AIS) · Data mining

Introduction

Low-carbon and green development has become the trend of global economic development nowadays, and "carbon peak" and "carbon neutrality" have been written into the Government Work Report in early 2021 for the first time (Government Work Report, 2021). Industries are making the transition to a low-carbon economy. This is especially true for shipping, one of the fastest growing industries in carbon emissions. China is the second largest shipowner in the world (International Ship Network, 2021), which plays a vital role in the decarbonization process of the shipping industry. Comprehensively improving the efficiency and level of atmospheric emission supervision from ships is beneficial: it can guide shipping enterprises to conduct emission reduction management on ships, helping China implement the great decision of "carbon peak" and "carbon neutrality"; it will help accelerate all-round green transformation of shipping trade and promote high-quality development; it will contribute to reducing major pollutants and greenhouse gas (GHG) emissions and achieve synergies in reducing pollution and carbon emissions; it will help advance the global climate governance process and demonstrate the sense of responsibility of a responsible major country, so as to enhance China's voice in the field of global energy conservation and emission reduction in shipping trade transportation. China has contributed its wisdom, solutions, and strength to the global climate governance process, demonstrating its responsibility and commitment to building a community with a shared future for mankind (Wang et al., 2021).

Responsible Editor: V.V.S.S. Sarma

✉ Qiang Mei
meiqiang@jmu.edu.cn

[1] Merchant Marine Academy, Shanghai Maritime University, Shanghai 200210, China

[2] Institute of Computing Technology Chinese Academy of Sciences, Beijing 100190, China

[3] Beijing University of Technology, Beijing 100124, China

[4] Jimei University, Xiamen 361021, China

The shipping industry is the lifeblood of the global trade economy, carrying more than 85% of the world's cargo (Robinson, 2002; Liu et al., 2014). As a powerful country in water transport, domestic shipping has become the main and key part of China's freight transport system (Tiwari et al., 2003). Against the background of "carbon peak" and "carbon neutrality," the Chinese government encourages freight transport to shift from road to water, which causes less pollution. Thus, domestic shipping is further developed. According to the International Convention for the Prevention of Pollution from Ships (MARPOL) issued by the International Maritime Organization (IMO) in 1973 (International Maritime Organization, 1973), contracting states shall undertake to give effect to the provisions of the articles of this convention and its by-laws under which it is obliged, so as to prevent pollution of the marine environment through the discharge of hazardous substances in violation of the convention or waste liquids containing such substances (Ye, 2015; Liu, 2009; Zhang and Lou, 2015; Liu et al., 2021a; Zhang et al., 2021). According to the third Greenhouse Gas Report released by the IMO in 2014, the global shipping industry emitted an average of 10.15 million tons of carbon dioxide per year from 2007 to 2012, accounting for 3.1% of global carbon emissions. It is estimated that total GHG emissions from the global shipping industry could increase by 50–250% by 2050 if no effective measures are taken. Therefore, on April 13, 2018, the 72nd meeting of the Marine Environmental Protection Committee (MEPC) adopted the GHG emission reduction strategy, which mainly includes seven aspects, including vision, emission reduction intensity, guiding principles, and short-, medium-, and long-term emission reduction measures. Moreover, developing countries were aided in completing their emission reduction strategies through measures such as technical cooperation and capacity building (Yue, 2018; Liu et al., 2021b). Meanwhile, in 2018, for the first time in shipping history, the European Union started monitoring carbon dioxide emissions from ships, according to regulations passed (Ren, 2014; Tan et al., 2021). It can be seen that the issue of carbon emissions from maritime ships has become the focus of increasing attention of the international community and countries in recent years (Brodie et al., 2017).

At present, there are two main international calculation methods for pollutant emissions from ships (He et al., 2021): the calculation method based on fuel consumption (Endresen et al., 2003; Endresen et al., 2005; Endresen et al., 2007; Hulskotte and Van Der Gon, 2010) and the dynamic method based on automatic identification system (AIS) data (Jalkanen et al., 2009; Jalkanen et al., 2012; Jalkanen et al., 2016; Wen et al., 2015; Nunes et al., 2017). Despite the use of fuel consumption-based methods to gather data, the comprehensive and accurate nature of this data has yet to be validated. In contrast, the dynamic method of estimating pollutant emissions is more reasonable in the selection of emission factors and more precise in the estimation of exhaust emissions. The European Environment Agency analyzed a detailed inventory of pollutant emissions from ships off the European coast from 1990 to 2017 and optimized the compilation method of emission inventory in practice (European Environment Agency, 2019). Chen et al. (2016) summarized the research results of the air pollutant emission inventory of ships at China's ports before 2016. Based on this, we summarized and analyzed the relevant research in the past 3 years, as shown in Table 1.

Existing research results show that the dynamic method based on AIS data is used by most scholars, and this method is feasible. However, the following problems still exist in current studies (Peng et al., 2020; Nandan and Rosen, 2009):

1. The dynamic method relies on high AIS data quality. Due to the problems of incomplete coverage of AIS base stations, blocked uplink signals of ships, and atmospheric radio interference on the system, AIS data can be missed, mistaken, and repeated, influencing the accuracy of this method.
2. Narrow research scope of pollutant discharge from ships. Current research is mainly limited to the emission inventory and emission characteristics of ports and specific areas, investigating the pollution of ports' surrounding environment. However, there is a lack of research on emissions from ships entering our territorial waters. It cannot effectively reflect the impact of environmental pollution within the territorial waters, failing to provide accurate statistics and analysis of carbon emissions from ships.
3. Lack of macro-control of pollutant discharge from ships. Current studies on shipping networks focus on the importance and status of ports and channels, but do not consider the impact of environmental pollution on them. Thus, we are unable to master the carbon emissions macroscopically and unable to fully formulate effective control plans, and the construction of green ports and ecological channels lacks data support.
4. Lack of research on ship carbon emission tracking and traceability. At present, the research on ship pollutant emissions focuses on the generation and pollutants of ship emissions, and there is no correlation research on ship nationality, right of ownership, right of use, and other attributes. Thus, we cannot manage the actual controllers and entities of the ship or grasp the cause and effect of ship emissions, and it cannot provide data support for China to formulate accurate carbon emission reduction policies and carbon trading.

The primary source of ship carbon emissions is the combustion of fossil fuels during sailing and operation. This

Table 1 Relevant research in the past 3 years

Authors	Calculation method	Study area	Research content
Huang et al. (2019)	AIS dynamic method	Shenzhen Port	Dynamic real-time statistical analysis system of ship exhaust emission
Peng et al. (2020)	AIS dynamic method	Yantian Port	Combined with ship navigation and emission characteristics, the Gaussian smoke diffusion model was established to analyze the diffusion characteristics of ships under different environmental parameters
Liu et al. (2020)	AIS dynamic method	Xiamen Port	The models of pollutant emission and diffusion from ships under different working conditions were constructed by geographic information system (GIS) technology
Liu et al. (2021c)	AIS dynamic method	Circum-Bohai Sea Economic Zone	Compiled an inventory of air pollutant emissions from ships
Zhang et al. (2020)	AIS dynamic method	Coastal Guangdong areas	AIS trajectories were used to calculate emissions
Wang et al. (2019)	AIS dynamic method and fuel consumption method	Shanghai Port	AIS dynamic method and fuel consumption method were combined to calculate energy consumption and emission inventories for various navigational states, fleet sizes, and spatiotemporal scales
Lv et al. (2019)	AIS dynamic method	Qingdao Port	The emission inventory was compiled, and the spatial emission characteristics, emission characteristics of different ship types, and emission characteristics under different working conditions were analyzed
Zeng et al. (2020)	AIS dynamic method	Xiamen Port	The emission inventory was compiled
Wang et al. (2020)	AIS dynamic method	Xiamen Port	The emission inventory was compiled, and the spatiotemporal distribution characteristics were analyzed
Zhang et al. (2019)	AIS dynamic method	Main lines of the Yangtze River	Combined with the navigational distribution characteristics of main lines of the Yangtze River, the section integral was introduced to calculate exhaust emissions from ships in cross sections
Li and Zhou (2021)	AIS dynamic method	Gaolan Port, Zhuhai	The emission inventory was compiled
Zhu et al. (2019)	AIS dynamic method	Yangtze River in Jiangsu Province	Emission inventory; spatiotemporal distribution characteristics; ship emission sharing rate
Xu et al. (2019)	AIS dynamic method	Yangtze River in Jiangsu Province	Emission inventory; spatiotemporal distribution characteristics; different ship types, operating conditions, and emission characteristics of power units
Yuan et al. (2020)	AIS dynamic method	Yangtze River in Jiangsu Province	Emission inventory; ship channel emissions; spatial distribution characteristics
Wan et al. (2020)	AIS dynamic method	China waters	Emission inventory; spatiotemporal distribution characteristics; ship type; sharing rate of operating conditions

paper employs big data analysis techniques to clean, fuse, and complete the AIS and Lloyd's data of ships. This process ensures high accuracy in the AIS data and eliminates the influence of erroneous AIS data on subsequent analyses. Using the dynamic method, this study calculates the PM_{10}, $PM_{2.5}$, NO_x, SO_x, and CO_2 emissions from the main engine, auxiliary engine, and boiler of various types of ships entering the waters near Tianjin Port from different countries. The analysis includes dry bulk carriers, container ships, roll-on/roll-off ships, oil product ships, and fishing boats and is conducted using pollutant emission parameters and other relevant data. This study addresses the lack of accurate statistics and analysis of ship emissions in Chinese territorial waters. By analyzing the pollution problems in the territorial waters and considering the impact of pollutant emissions from ships, the study provides a comprehensive and macroscopic perspective on the issue. The analysis also fills the gap in accurate statistics and provides a comprehensive understanding of the emissions from ships entering Chinese territorial waters.

By conducting a fine-grained analysis of the time and location of pollutant emissions generated by ships and examining the specific attributes of ships in Tianjin Port, this study can accurately trace the source of pollutant emissions from ships. The study also includes a correlation analysis of ship nationality, ownership, and use rights to gain a comprehensive understanding of the causation and effect of pollutants. The findings of this study facilitate the effective management of ship entities, offering valuable references for the development of the Chinese shipbuilding industry and

Table 2 Sailing states of ships

Speed	Ship state	Description
< 1 knot	Docking	Docking should be judged together with the ship's position, as the velocity of ships in anchorage is sometimes less than one knot
1 < speed ≤ 3	Mooring	
3 < speed ≤ 20% of maximum continuous speed	Maneuvering operation	
20% of maximum continuous speed < speed ≤ 65% of maximum continuous speed	Low steaming	
Speed > 65% of maximum continuous speed	Cruise	

the standardization of shipbuilding technology. Our study can assist relevant departments in implementing stricter controls in areas that commonly violate pollutant emission regulations.

Moreover, it provides insights into the spatial and temporal emission patterns of pollutant emissions from ships, which can aid in improving emission standards and management for different seasons and times. The findings can also inform the development of management fee policies for different trades. It promotes the development of green ports, green ships, zero-carbon ports, and ecological channels (Wang et al., 2020). This will help to accelerate the restructuring of transportation and promote coordinated efforts to reduce pollution and carbon emissions. By providing supporting data for China to formulate accurate carbon emission reduction and carbon trading governance policies, the findings of this study can help achieve a dynamic balance between transport service supply and green demand at a higher level (Wen et al., 2017; Chen et al., 2014).

Materials and methods

Based on ships' AIS data, this paper selects ships, including dry bulk carriers, container vessels, roll-on/roll-off ships, oil tankers, and fishing vessels, from various countries by using shipping trajectories and geographic information. The dynamic method is used to study the pollutant emission from the ship's main engine, auxiliary engine, and boiler while in cruise, low steaming, maneuvering operation, and mooring during the period they enter the Tianjin Port until they depart. Thus, the pollutant emissions of these ships into China can be estimated.

Calculation model

Pollutant emission calculation model

Each piece of AIS data reflects the navigation state of the ship at a certain time, and the two pieces of AIS data of the same ship at adjacent moments can be considered to approximately reflect the navigation state of the ship at this period of time. The average sailing speed of two pieces of AIS data of the same ship at adjacent moments can be considered to represent the average sailing speed during this period. The sailing time of the ship in this distance can be obtained by the time difference of two adjacent AIS data of the same ship. We use the ship speed to judge its navigation state. The load factor of the main engine is calculated by the ratio of actual speed and designed speed. The load factors of the auxiliary engine and the boiler are determined by the ship sailing state and ship type.

The sailing state of the ship includes cruise, navigation in the deceleration zone, maneuvering operation, docking, and mooring. Generally, the working state of ship power equipment varies with the sailing state of the ship. Table 2 shows the distinguishing method of the ship's sailing state:

This paper adopts the dynamic calculation method using ships' AIS data, based on the functional relationship between the output energy of ship's main engine, auxiliary engine, and

Table 3 Pollutant emission factor of the ship's main engine (*EFi*) (g/kW·h)

Ship type	Year of build	PM_{10}	$PM_{2.5}$	DPM	NO_x	SO_x	CO	HC	CO_2	N_2O	CH_4
Low-speed diesel engine	≤ 1999	1.05	0.96	1.5	18.1	10.5	1.4	0.6	620	0.031	0.012
Medium-speed diesel engine	≤ 1999	1.11	1.02	1.5	14	11.5	1.1	0.5	683	0.031	0.01
Low-speed diesel engine	2000–2010	1.05	0.96	1.5	17	10.5	1.4	0.6	620	0.031	0.012
Medium-speed diesel engine	2000–2010	1.11	1.02	1.5	13	11.5	1.1	0.5	683	0.031	0.01
Low-speed diesel engine	2011–2015	1.05	0.96	1.5	15.3	10.5	1.4	0.6	620	0.031	0.012
Medium-speed diesel engine	2011–2015	1.11	1.02	1.5	11.2	11.5	1.1	0.5	683	0.031	0.01

Table 4 Low load adjustment factor of the ship's main engine *CF* (nondimensionalized)

Load factor (LF)	PM_{10}	$PM_{2.5}$	DPM	NO_x	SO_x	CO	HC	CO_2	N_2O	CH_4
1%	19.17	19.17	--	11.47	5.99	19.32	59.28	5.82	--	--
2%	7.29	7.29	7.29	4.63	3.36	9.7	21.18	3.28	4.63	21.18
3%	4.33	4.33	4.33	2.92	2.49	6.49	11.68	2.44	2.92	11.68
4%	3.09	3.09	3.09	2.21	2.05	4.86	7.71	2.01	2.21	7.71
5%	2.44	2.44	2.44	1.83	1.79	3.9	5.61	1.76	1.83	5.61
6%	2.04	2.04	2.04	1.6	1.61	3.26	4.35	1.59	1.6	4.35
7%	1.79	1.79	1.79	1.45	1.49	2.8	3.52	1.47	1.45	3.52
8%	1.61	1.61	1.61	1.35	1.39	2.45	2.95	1.38	1.35	2.95
9%	1.48	1.48	1.48	1.27	1.32	2.18	2.52	1.31	1.27	2.52
10%	1.38	1.38	1.38	1.22	1.26	1.97	2.18	1.25	1.22	2.18
11%	1.3	1.3	1.3	1.17	1.21	1.79	1.96	1.21	1.17	1.96
12%	1.24	1.24	1.24	1.14	1.18	1.64	1.76	1.17	1.14	1.76
13%	1.19	1.19	1.19	1.11	1.14	1.52	1.6	1.14	1.11	1.6
14%	1.15	1.15	1.15	1.08	1.11	1.41	1.47	1.11	1.08	1.47
15%	1.11	1.11	1.11	1.06	1.09	1.32	1.36	1.08	1.06	1.36
16%	1.08	1.08	1.08	1.05	1.07	1.24	1.26	1.06	1.05	1.26
17%	1.06	1.06	1.06	1.03	1.05	1.17	1.18	1.04	1.03	1.18
18%	1.04	1.04	1.04	1.02	1.03	1.11	1.11	1.03	1.02	1.11
19%	1.02	1.02	1.02	1.01	1.01	1.05	1.05	1.01	1.01	1.05
20%	1	1	1	1	1	1	1	1	1	1
> 20%	1	1	1	1	1	1	1	1	1	1

boiler (unit: kW·h) and the emission factors corresponding to various emissions multiplied, and the emission factors adopted in the calculation are grams per kilowatt hour·h as the measurement unit. Finally, the corresponding emission factor correction factor is used for correction.

The output energy of the ship's main engine, auxiliary engine, and boiler is different under different sailing states, and the calculation formula is as follows:

$$Energy = Load \times Act \tag{1}$$

where *Energy* refers to the energy consumed by a ship under different operating conditions (kW·h); *Load* represents the load power of the ship's main engine, auxiliary engine, or boiler under different operating conditions, and for the main engine, auxiliary engine, and boiler, the load calculation is different, so the energy consumption is different; and *Act* is the ship's sailing time (h).

Pollutant emissions from ships are calculated based on ships' output energy, as shown in Eq. (2):

$$Ei = Energy \times EF \times FCF \times CFi \tag{2}$$

where *Ei* is the emission of pollutants from different types of ships (g); *Energy* refers to the energy consumed by a ship under different operating conditions (kW·h); *EF* is the emission factor of this pollutant (g/kW·h); *FCF* is the fuel correction factor, a dimensionless unit; and *CFi* is the emission correction factor, a dimensionless unit.

Emission factors and parameters

Emission algorithms and parameters for the ship's main engine

The calculation formula for pollutant emissions from the ship's main engine is as follows:

$$Ei = MCR \times LF \times Act \times EFi \times FCF \times CF \tag{3}$$

Table 5 Fuel correction factor (*FCF*) (nondimensionalized)

Fuel	NO_x	VOC	CO	SO_x	PM_{10}	$PM_{2.5}$	DPM	CO_2	N_2O	CH_4
RO (2.7%S)	1	1	1	1	1	1	1	1	1	1
HFO (1.5%S)	1	1	1	0.56	0.82	0.82	0.82	1	1	1
MGO (0.5%S)	0.9	1	1	0.18	0.39	0.39	0.39	1	0.9	1
MDO (1.5%S)	0.9	1	1	0.56	0.47	0.47	0.47	1	0.9	1
MGO (0.1%S)	0.9	1	1	0.04	0.35	0.35	0.35	1	0.9	1

Table 6 The maximum speed of ships based on the type (knot)

Ship type	Average cruise speed	Maximum cruise speed (the average cruise speed is 94% of the maximum cruise speed)	Maximum cruise speed (rounding, carry bit)
Vehicle carrier	18.7	19.89362	20
Dry bulk carrier	14.5	15.42553	16
Container vessel	21.6	22.97872	23
Cruise ship	20.9	22.23404	23
General cargo ship	15.2	16.17021	17
Ocean tugboat	14.5	15.42553	16
Refrigerator ship	19.5	20.74468	21
Roll-on/roll-off ship	16.8	17.87234	18
Oil tanker	14.8	15.74468	16
Others	17.4	18.51064	19

where *Ei* is the emission of pollutants from different types of ships in the main engine (g); *MCR* is the maximum continuous rated power of the ship's main engine (kW); *LF* is the load factor of the ship's main engine, a dimensionless unit; *Act* is the ship's sailing time (h); *EFi* is the emission factor of this pollutant in the main engine (g/kW·h) (see Table 3); *FCF* is the fuel correction factor, a dimensionless unit (see Table 5); and *CF* is low load adjustment factor of the ship's main engine, a dimensionless unit (see Table 4).

$$LF = \left(\frac{Speed\_Actual}{Speed\_Maximum}\right)^3 \tag{4}$$

where *Speed_Actual* is the ship's actual speed (knot); *Speed_Maximum* is the ship's maximum designed speed (knot). When the maximum designed speed is not recorded in the database, classifications in Table 6 can be used for selection. The emission parameters of the main engine are listed as follows.

Emission algorithms for the ship's auxiliary engine

The calculation formula for pollutant emissions from the ship's auxiliary engine is as follows:

$$Eai = A\_MCR \times LF\_a \times Act \times EFai \times FCF\_a \tag{5}$$

where *Eai* is the emission of certain types of pollutant from the ship's auxiliary engine (g); *A_MCR* is the maximum continuous rated power of the ship's auxiliary engine (kW); *LF_a* is the proportional coefficient of load factor of the ship's auxiliary engine, a dimensionless unit (see Table 8); *Act* is the running time of the ship's auxiliary engine (h); *EFai* is the emission factor of this pollutant in the ship's auxiliary engine (g/kW·h) (see Table 9); and *FCF_a* is the fuel correction factor, a dimensionless unit (see Table 10).

$$A\_MCR = AMR \times MCR \tag{6}$$

where *AMR* is the ratio of the power of the auxiliary engine to the maximum continuous rated power of the main engine. Thus, the power of the ship's auxiliary engine can be calculated (see Table 7).

Parameters related to auxiliary engine emissions are listed in the following tables:

Emission algorithms for the ship's boiler

The calculation formula for pollutant emissions from the ship's boiler is as follows:

$$Ebi = B\_Energy \times Act \times EFbi \tag{7}$$

where *Ebi* is the emission of certain types of pollutants from the ship's boiler (g); *B_Energy* refers to the load power of the ship's boiler (kW) (see Table 11); *Act* is the running time of the ship's boiler (h); and *EFbi* is the emission factor of pollutants in the ship's boiler (g/kW·h) (see Table 12).

Table 7 The ratio of the power of the auxiliary engine to the maximum continuous rated power of the main engine (*AMR*)

Ship type	*AMR*
Vehicle carrier	0.266
Dry bulk carrier	0.222
Container vessel	0.22
Cruise ship	0.278
General cargo ship	0.191
Ocean tugboat	0.256
Refrigerator ship	0.406
Roll-on/roll-off ship	0.259
Oil tanker	0.211
Others	0.256

Table 8 The proportional coefficient of load factor of the ship's auxiliary engine (*LF_a*)

Ship type Ship state	Cruise	Low steaming	Maneuvering operation	Docking	Mooring
Vehicle carrier	0.15	0.3	0.45	0.26	0.26
Dry bulk carrier	0.17	0.27	0.45	0.22	0.22
Container vessel	0.13	0.25	0.5	0.17	0.17
Cruise ship	0.8	0.8	0.8	0.64	0.64
General cargo ship	0.17	0.27	0.45	0.22	0.22
Ocean tugboat	0.17	0.27	0.45	0.22	0.22
Refrigerator ship	0.2	0.34	0.67	0.32	0.32
Roll-on/roll-off ship	0.15	0.3	0.45	0.3	0.3
Oil tanker	0.24	0.28	0.33	0.26	0.26
Others	0.17	0.27	0.45	0.22	0.22

Shipping emission inventory

Study area and data sources

The study area for this research is the sea area near Tianjin Port, as shown in Fig. 1. The points depicted on the right-hand side of the figure represent the navigating points of vessels in the study area (Chen and Lu, 2012). The study data used in this research include AIS data and archival data of ships from various countries that entered the Tianjin Port channels during the second half of 2018. The ships analyzed in this study include oil tankers, container vessels, dry bulk carriers, passenger ships, roll-on/roll-off ships, and fishing vessels. The pollutants studied in this research are PM_{10}, $PM_{2.5}$, NO_x, SO_x, and CO_2 emissions from these ships.

The input data are divided into three parts, namely, the ship's static Lloyd's data, the real-time dynamic AIS data, and pollutant emission parameter data. AIS sends signals at regular intervals, ranging from every 3 s to a few minutes, providing detailed information on ship speed and position. High-precision AIS data ensure the accuracy of ship emission calculations.

Pollutant emission parameters are fixed, including ship state judgment conditions. In this research method, the real-time ship speed is used to judge whether the ship is in the state of docking, mooring, maneuvering in ports, slowing down, or cruise. The emission parameter data contain the speed threshold to judge the ship state. In addition, the data contain load factors of main engine, auxiliary engine, and boiler in different working conditions, pollutant emission factors of the main engine of different types of ships and years of build, fuel correction factors, ratios of the power of the auxiliary engine to the maximum continuous rated power of the main engine of different types of ships, pollutant emission factors of the auxiliary engine of ships with different years of build, and pollutant emission factors of the ship's boiler. Since the pollutant emission parameter is fixed, it is written into the program files AMR.py, B_Act.py, B_ENERGY.py, FCF.py, EFAI.py, EFBI.py, EFI.py, LF_A.py, and SHIP_STATE.py. Moreover, relevant access methods are defined to use them directly.

In this paper, the extended data of pollutant emissions from the standing book of all Tianjin ports in June, July, August, October, November, and December, 2018 are used, which include Lloyd's data and AIS data. The former is used as the ship's static information database, and the latter is used as real-time dynamic AIS data of ships. All data in the form of XLSX files are subjected to a series of work, including data preprocessing, data fusion, and data calculation.

The ship's static Lloyd's data include the basic information of the ship, e.g., maritime mobile service identify (MMSI), year of build, ship nationality, maximum rated power of the main engine, maximum designed speed, fuel type, maximum rated power of the auxiliary engine, and ship type. For missing data, default values are used to complete. The default value is obtained by means of statistical average, but missing data for the ship nationality is identified as unknown.

In this experiment, the dynamic method is used to calculate the amount of ship emission. That is, based on the

Table 9 The emission factor of pollutants in the ship's auxiliary engine (*EFai*) (g/kW·h)

Year of build	PM_{10}	$PM_{2.5}$	DPM	NO_x	SO_x	CO	HC	CO_2	N_2O	CH_4
≤ 1999	1.11	1.02	1.5	14.7	12.3	1.1	0.4	683	0.031	0.01
2000–2010	1.11	1.02	1.5	13	12.3	1.1	0.4	683	0.031	0.01
2011–2015	1.11	1.02	1.5	11.2	12.3	1.1	0.4	683	0.031	0.01

Table 10 The fuel correction factor in the auxiliary engine (*FCF_a*) (nondimensionalized)

Fuel	NO_x	VOC	CO	SO_2	PM_{10}	$PM_{2.5}$	DPM	CO_2	N_2O	CH_4
RO (2.7%S)	1	1	1	1	1	1	1	1	1	1
HFO (1.5%S)	1	1	1	0.56	0.82	0.82	0.82	1	1	1
MGO (0.5%S)	0.9	1	1	0.18	0.39	0.39	0.39	1	0.9	1
MDO (1.5%S)	0.9	1	1	0.56	0.47	0.47	0.47	1	0.9	1
MGO (0.1%S)	0.9	1	1	0.04	0.35	0.35	0.35	1	0.9	1

real-time operating state and shipping trajectory of the ship, the carbon emissions in China's territorial sea and ports are analyzed by using the energy output from the ship's main engine, auxiliary engine, and boiler. The time difference between two adjacent moments is extracted from AIS data, and the information on ship navigational state and load coefficient is judged according to ship speed, sailing distance, and other data in this period. Thus, the pollutant emission of the main engine, auxiliary engine, and boiler can be calculated. The required ship design speed, ship type, and other information can be obtained according to the MMSI of the ship in AIS data. Therefore, AIS data should include real-time data such as ship sailing time, latitude and longitude coordinates, heading, and speed. The extended data of pollutant emissions from the standing book of all channels in the surrounding area of Tianjin Port are selected. After data preprocessing, the extracted data are used as the dynamic AIS data of ships in this research method.

Data processing

In this paper, the dynamic method is adopted to calculate pollutant emissions from ships, which makes the quality of AIS data crucial in determining the accuracy of the research results.

AIS is a navigational tool that contains a large amount of information about the ship. This information can be extracted and analyzed to understand the ship's navigation status. The AIS transponders broadcast detailed information about the ship's speed and position at regular intervals, ranging from every 3 s to a few minutes, and the high accuracy of AIS data ensures the accuracy of the ship's emission calculation. The quick transmission of AIS data allows the ship to obtain multiple AIS data from other ships in a short period. Therefore, the dynamic information provided by the AIS of ships can be used to calculate emissions accurately. During the process of using equipment, transmitting, and collecting data, the AIS data may suffer from issues such as missing information, errors, repetitions, and anomalies. These issues can arise due to various factors, such as the characteristics of the sensors, signal interference, and congestion in the transmission channels (Wu et al., 2017). Therefore, preprocessing of AIS data is necessary to mitigate the potential impact on analysis outcomes. Data preprocessing involves cleaning, integrating, fusing, and completing data to eliminate errors so that high accuracy of AIS data and emission inventory can be achieved.

Table 11 The load power of the ship's boiler (kW)

Ship type Ship state	Cruise	Low steaming	Maneuvering operation	Mooring
Vehicle carrier	0	0	371	371
Dry bulk carrier	0	0	109	109
Container vessel	0	0	506	506
Cruise ship	0	0	1393	1393
General cargo ship	0	0	137	137
Ocean tugboat	0	0	0	0
Refrigerator ship	0	0	109	109
Roll-on/roll-off ship	0	0	464	464
Oil tanker	0	0	371	3000
Others	0	0	137	137

Data cleaning

Since possible faults, errors, discontinuities, and other problems may occur in storage and management of massive AIS data and the process of multi-channel incremental AIS data access may encounter problems such as data missing, anomaly, brevity, and unstable rate, the big data analysis technique is used. According to the demand for carbon emission traceability of ships, it is utilized for extraction so as to achieve satisfactory analysis results. Data processing is illustrated in Fig. 2.

The anomalous ship speed is judged by comparing the real-time ship speed with the maximum ship speed. If the former is greater than the latter, the track points will be removed as anomalous speed. The ship heading angle ranges from 0 to 360°, and if the heading angle exceeds the normal range, the track points will be removed as anomalous heading angle. According to China's land map and inland river map, we delimit the research scope of the ship's track points as shown in Fig. 1. If the position of the ship's track point falls within the mainland of China, the track points will be removed as anomalous position. Moreover, according to the IMO number of the ship, the ship name, the reporting time,

Table 12 The emission factor of pollutants in the ship's boiler (g/kW·h)

PM_{10}	$PM_{2.5}$	DPM	NO_x	SO_x	CO	HC	CO_2	N_2O	CH_4
0.8	0.64	0	2.1	16.5	0.2	0.1	970	0.08	0.002

and other information, we eliminate the repeatedly reported AIS information (Zong et al., 2012). The anomaly data processing is tabulated in Table 13.

Data fusion

Lloyd's data include ship type, maximum cruising speed, maximum continuous rated power of ship's main engine, year of build, ship's main engine type, fuel type, and main engine speed (high-speed machine: greater than 1000 rpm; medium-speed machine: $300 < n \leq 1000$ rpm; low speed machine: ≤ 300 rpm). AIS data record the actual sailing speed of the ship, ship sailing time (starting and ending time of various sailing states), and ship sailing state. Through the MMSI code provided by the AIS static database, ship engine power, ship load, ship speed, and other ship information can be found in Lloyd's database.

Data completion

For the data not included in this database, the method of fitting relation calculation or statistical average is used for determination. Finally, a complete data database of ship pollutant emissions is established.

Results and discussion

This study is aimed at analyzing the sources of pollutant emissions, especially carbon emissions, from ships in the vicinity of Tianjin Port. The dynamic method is employed to calculate ship pollutant emissions using static data of pollutant emission parameters, Lloyd's data, and dynamic AIS data of ships. This approach allows for the construction of a detailed emission inventory that includes information on the time, location, country of origin, type, and navigation status of the emitting ships. By analyzing emission sources and characteristics, this study can accurately trace pollutant emissions from ships, including information on the nationality, ownership, and use rights of the ships.

Moreover, the proposed method addresses the lack of accurate statistical data and allows for a comprehensive analysis of ship emissions within the Chinese territorial waters and the resulting pollution problems. The proposed method provides a comprehensive assessment of the pollution situation caused by ship emissions, allowing for a macro-level analysis from various perspectives. This information can be used to inform the development of China's shipbuilding industry, regulate shipbuilding technology, and implement stricter control measures in areas that commonly violate pollutant emission regulations.

This approach can facilitate the development of emission standards and management policies that are tailored for specific seasons, times, and trades. Moreover, it can promote the development of green ports, green ships, zero-carbon ports, and ecological corridors and facilitate the acceleration of transportation structure adjustments. Carbon trading can be established in China based on the data obtained from this study, which can facilitate the establishment of targeted carbon emission reduction policies. This will provide robust support for achieving a dynamic balance between the supply of transportation services and the green demand at a higher level.

Temporal distribution law

This study focuses on the analysis of pollutant emissions from ships in the vicinity of Tianjin Port from June to

Table 13 The anomaly data processing

Anomaly classifier	Anomaly type	Anomaly characteristics	Cleaning method
Data anomaly	Outlier	Data field, MMSI, IMO, ship name, and ship type exceed the threshold	Removed or corrected
	Data missing	Missing fields, data, or trajectories	Removed or completed
Behavior anomaly	Anomalous movement	The ship speed and heading exceed the threshold	Removed
	Anomalous trajectory	Destination mismatch, trajectory termination, and abnormal shape	Removed or cut
Position anomaly	Based on historical trajectory	The ship's position is not consistent with its historical trajectory	Removed
	Based on the map	The ship deviates from the course, location on land, etc.	Removed

Table 14 Pollutant emissions of areas near Tianjin Port in the second half of 2018 (g)

	June	July	August	September	October	November	December
PM_{10}	5623994	6239469	6321762	6972860	7032996	6670809	6037294
$PM_{2.5}$	5162705	5727277	5802757	6399844	6455774	6123435	5542137
NO_x	65723346	72056027	73244611	80158307	80621560	76768196	69652644
SO_x	57462040	63250624	64043380	70387685	70726000	67327722	61304130
CO_2	3269170301	3533871474	3354522556	3421613901	3469552052	3318947963	3216805883

December 2018. An example of calculation results is shown in Table 14.

The broken line chart of total pollutant emissions from ships in the waters near Tianjin Port from June 2018 to December 2018 is provided in Fig. 3.

It is evident that CO_2 emissions are more concentrated in August, September, and October; peak in July; and are distributed less in June and December. This is because the fishing season is closed in June in the Bohai Bay area, where strict ship controls are practiced. In December, sea ice in the north affects navigation to some extent. The emission trend of other pollutants remains basically consistent, with the lowest emissions in June due to the impact of the fishing ban period. However, emissions are primarily concentrated in September, October, and November.

Spatial distribution law

The longitude and latitude of the study area range from 117.35° E–118.35° E and 38.64° N–39.24° N. The ship's longitude and latitude information provided by the AIS data is used to combine the real-time emissions of the ship with the actual sailing route of the ship. The spatial distribution of ship carbon emissions in Tianjin Port in the second half of 2018 was drawn by GIS technology, as shown in Fig. 4.

In Fig. 4, the red area represents the channel, and the purple area denotes the anchorage. As can be seen from Fig. 4, atmospheric carbon emissions from ships are mainly concentrated near the land port area of Tianjin Port and on the channels. Tianjin Port is divided into Beijiang Port Area, Dongjiang Port Area, Nanjiang Port Area, Dagukou Port Area, Gaoshaling Port Area, Dagang Port Area, Haihe Port Area, and Beitang Port Area. It is obvious that the pollutant emissions in the Main Shipping Channel of Tianjin Xingang Fairway and Dagusha Channel are significantly higher than in other channels.

Ship nationality list

Ship nationality is an important aspect of carbon emission source research, which is conducive to the attribution of tax entities of carbon emission trading. Taking carbon emissions as an example and after fusing AIS data and ship archival data, the nationality and registration place of ships near Tianjin Port in the second half of 2018 are studied. The total emissions of PM_{10}, $PM_{2.5}$, NO_x, SO_x, and CO_2 in different months are tabulated in Table 15.

The proportion and ranking of different countries'/regions'carbon emissions are presented in Fig. 5 and Table 16, respectively.

According to the analysis presented in Fig. 5 and Table 16, it can be observed that ships registered in China have the highest carbon emissions to China, followed by those registered in Hong Kong, China. Ships registered in Liberia and Singapore follow next in terms of carbon emissions to China. Ships from the Chinese mainland account for 60.7% of carbon emissions, while those from Hong Kong, China, account for 7.2%. This finding suggests the need for coordinated efforts among relevant departments to manage emissions from ships. It is important to not only strictly regulate emissions from local ships but also monitor and manage the port activities of ships from other regions. Carbon emission data can be used to inform the taxation of carbon

Table 15 Pollutant emissions of areas near Tianjin Port in the second half of 2018 (g)

Nationality Month	June	July	August	September	October	November	December
China	84733059.7	90928328.03	92161375.4	104103423	101277248.9	95674656.26	86640743.22
Marshall Islands	3649140.49	5334805.878	3820734.924	2789110.92	3088766.17	4874812.226	5170079.456
Liberia	5085633.241	6709654.51	7216887.967	7144252.446	6780516.827	7290068.296	7293692.604
Hong Kong, China	9618547.386	10238692.25	12776571.4	13983607.67	13398541.06	12346794.67	11813919.59
Singapore	3028707.892	3370841.908	3773008.441	5744557.501	5218711.83	5873331.887	4498342.493

Table 16 Carbon emission ranking of ships of different nationalities

Month	First place	Second place	Third place
June	China	Marshall Islands	Hong Kong, China
July	China	Hong Kong, China	Singapore
August	China	Hong Kong, China	Liberia
September	China	Hong Kong, China	Singapore
October	China	Hong Kong, China	Singapore
November	China	Hong Kong, China	Liberia
December	China	Hong Kong, China	Liberia

emission trading rights for ships, making it an effective tool for promoting green shipping practices.

Ship type

The amount of carbon emitted by different ship types is different, so this section mainly takes carbon emissions as an example to analyze the emission characteristics of different types of ships. Carbon emissions of dry bulk carriers, container vessels, oil product carriers, tugboats, relief ships, fishing vessels, and roll-on/roll-off ships are shown in Table 17.

By analyzing the emission inventory, the pollutant sharing rate of each ship type is shown in Fig. 6.

It is evident that dry bulk carriers, container vessels, oil product carriers, and tugboats emit higher levels of GHGs compared to other types of vessels. These vessel types account for a significant proportion of total GHG emissions, with a combined emission sharing rate of 81.54%. These ship types are the mainstay of current shipping, with dry bulk carriers having the highest GHG emission sharing rate of 32.64%, followed by container vessels (24.48%), oil product carriers (12.3%), and oil product ships (12.11%).

Based on the analysis, it is found that dry bulk carriers have the highest carbon emissions among all ship types, followed by container vessels. Other types of vessels have relatively low carbon emissions. Table 18 shows the arrival of various types of ships from the perspective of the number of vessels.

Tianjin Port is the largest port in northern China and the gateway to Beijing's shipping trade, which is a comprehensive international port with complete cargo categories. It is one of the largest comprehensive ports around the Bohai Sea, and it has formed a cargo source structure with containers, crude oil and products, ore, and coal as the "four pillars" and steel and grain as "a group of key points." It is a trunk container port in northern China, with a large number of container vessels. Container vessels have high speed, heavy loads, and much greater engine power than other types of ships, and the emission of pollutants from a container vessel is much higher than from other types of ships. It is found that there is no significant difference in the single-ship pollutant emissions of dry bulk carriers compared to other types of ships. However, the number of dry bulk carriers accounts for approximately 30% of the total number of ships. As it has the largest number of all ship types, container vessels emit pollutants second only to dry bulk carriers. Figure 7 presents the distribution of pollutants emitted by different types of ships from June to December in 2018.

As shown in Fig. 7, the exhaust emission rates of fishing vessels, dry bulk carriers, container vessel, pilot vessels, passenger ships, cruise ships, and law enforcement vessels are more concentrated in August, September, and October; peak in September; and gradually decrease in November and December. Contrastingly, the exhaust emission rates of tugboats and oil product carriers are the lowest in September and gradually increase in the following months.

Ship sailing state

In this study, the ship movement process is divided into four modes according to the ship's sailing speed: working conditions of cruise, low steaming, maneuvering operation, and mooring. In Table 19 shown in this subsection, we analyze the emission characteristics of ships in different navigation states using carbon emissions as an example. The ship's main engine provides power for navigation, and the propeller drives the ship by absorbing the power provided by the main engine. Thus, the main engine must be started in cruise, low

Table 17 Carbon emissions of different ship types (g)

Ship type	Main engine	Auxiliary engine	Boiler	Total emissions
Dry bulk carrier	5,619,272,835	2,072,823,913	7,914,055.4	7,700,010,803
Container vessel	5,055,497,001	717,938,819.5	353,390.4	5,773,789,211
Oil product carrier	1,815,937,153	1,041,246,166	437,208.1	2,857,620,527
Tugboat	1,138,927,184	480,648,658.5	0	1,619,575,842
Relief ship	619,580,922.4	460,425,069.8	61,129.4	1,080,067,122
Fishing vessel	538,585,734.8	455,421,744.5	31,371,342.3	1,025,378,822
Roll-on/roll-off ship	498,500,193	128,532,940.2	0	627,033,133.2

Table 18 The number of various types of ships arriving at Tianjin Port

Month	Dry bulk carrier	Oil product carrier	Container vessel	Tugboat	Relief ship	Fishing vessel	Roll-on/roll-off ship
June	1048	390	198	221	181	86	56
July	1131	425	192	245	171	188	49
August	1099	431	184	239	196	225	49
September	1005	432	182	241	180	561	41
October	1029	459	197	236	169	467	48
November	1055	445	170	273	200	343	42
December	872	417	187	239	212	278	41

steaming, and maneuvering operation states, and the carbon emission is the largest. The ship's auxiliary engine mainly provides electric energy for navigation. As the study area selected in this study is close to the port, the average sailing speed of the ship is lower than that of the ship running at sea, which leads to a decrease in the emission ratio of the ship's main engine and an increase in the emission ratio of the auxiliary engine. The carbon emission of the auxiliary engine accounts for about 1/3 of the total emissions and is also the main source of ship carbon emissions. The boiler is mainly started when the main engine is under low load and is used to provide heat for the normal operation of the ship. The load power and emission factor of the boiler are much smaller than those of the main engine and auxiliary engine. Hence, in general, the carbon emission of the boiler is smaller than that of the main engine and auxiliary engine.

In 2018, there were 31,768 pieces of AIS data, including 7161 pieces of state 0, 23,337 pieces of state 1, 163 pieces of state 2, 888 pieces of state 3, and 219 pieces of state 4, where 0 represents cruise, 1 denotes low steaming, 2 stands for maneuvering operation in the port, 3 means mooring, and 4 indicates docking.

When the ship sails at sea, the boiler is in the closed state. When the ship is in the cruise state or low steaming state, the boiler load power is 0. Therefore, many boiler carbon emissions are 0 in the estimation results. When the ship is in the cruise or low steaming, the ship is in the channel. When the ship is in the state of maneuvering operation and berthing, the ship is mostly located in the anchorage and berth, and carbon emissions are generated by auxiliary engines and boilers. The berthing time of ships accounts for about 70% of the total time (Liu, 2018), so the carbon emission is higher in the berthing state. Under the maneuvering operation, the ship has lower speed and shorter sailing time, and the pollutant emission proportion is the lowest. Berthing state is the driving state with the highest contribution to carbon emissions; hence, the carbon emissions near the harbor basin account for a significantly higher proportion than other pollutants.

Conclusions

Ship exhaust emission is one of the main sources of air pollution in port cities. This paper uses the calculation method based on ship power to study the carbon emission sources of ships in Tianjin Port and establishes the characteristics and inventory of ship carbon emissions in Tianjin Port in the second half of 2018. A series of problems occurring in methods based on ship fuel consumption have been solved. The AIS data undergo preprocessing including data cleaning, data fusion, and data completion to ensure accurate calculation. The carbon emission source and carbon input are analyzed accurately from three different dimensions: space-time distribution, ship attributes, and ship navigational states. This study has established a comprehensive understanding of the relationship between ship activities and carbon emissions,

Table 19 Carbon emissions of the ship under different working states (g)

Sailing state	Main engine	Auxiliary engine	Boiler	Total emissions
Cruise	14,178,018,412	2,020,085,536	0	16,198,103,948
Low speed	14,373,200,865	7,826,528,804	0	22,199,729,669
Maneuvering operation	21,456,888.59	64,158,423.32	7,900,960.4	93,516,272.32
Mooring	46,209,396.35	187,968,179.8	48,129,838	282,307,414.5
Berthing	360,213.177	46,163,406.83	15,381,756	61,905,375.61

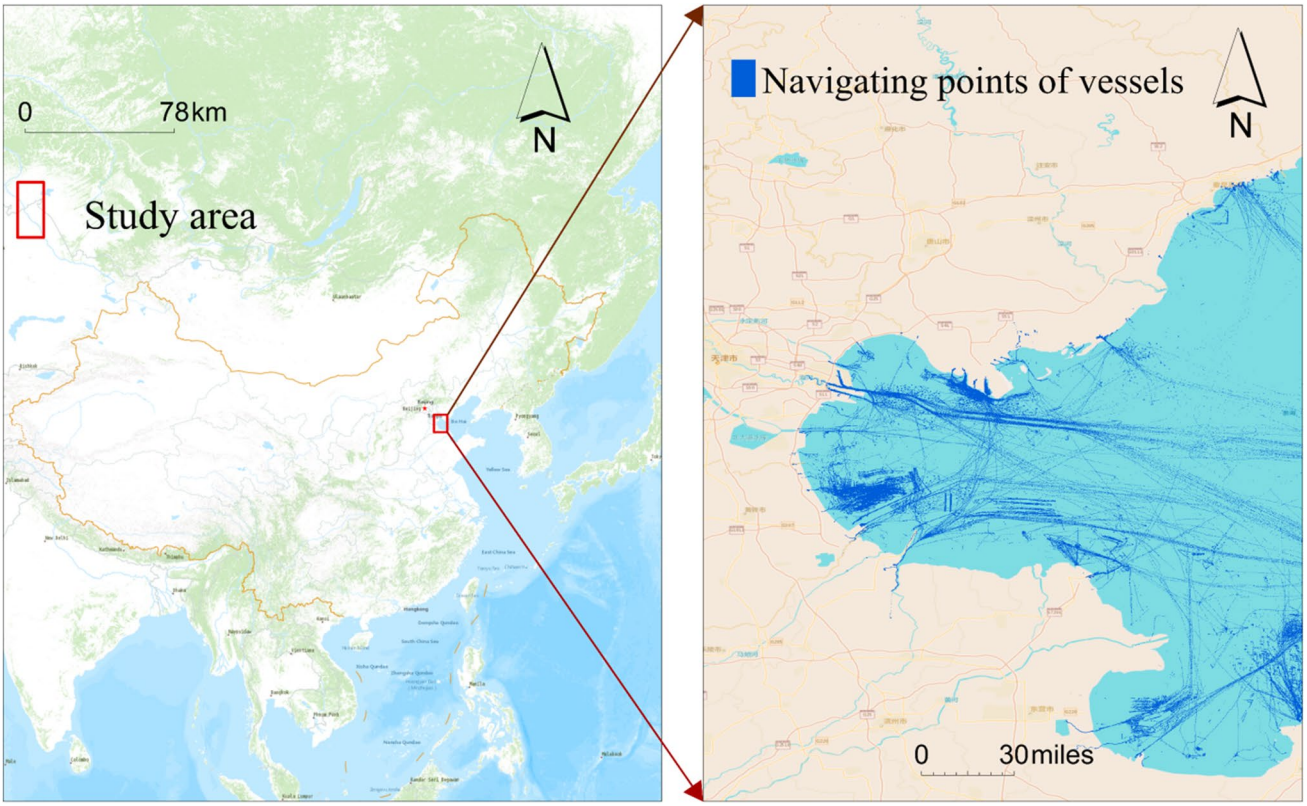

Fig. 1 The layout of Tianjin Port and navigating points of vessels

which can provide valuable data support for policy-making in emission reduction by relevant authorities. The main conclusions are obtained as follows.

The pollutant emissions in the region near Tianjin Port are mainly concentrated in the vicinity of Tianjin Port land port area, Dagusha Channel, and the Main Shipping Channel of Tianjin Xingang Fairway. Carbon emissions peak in

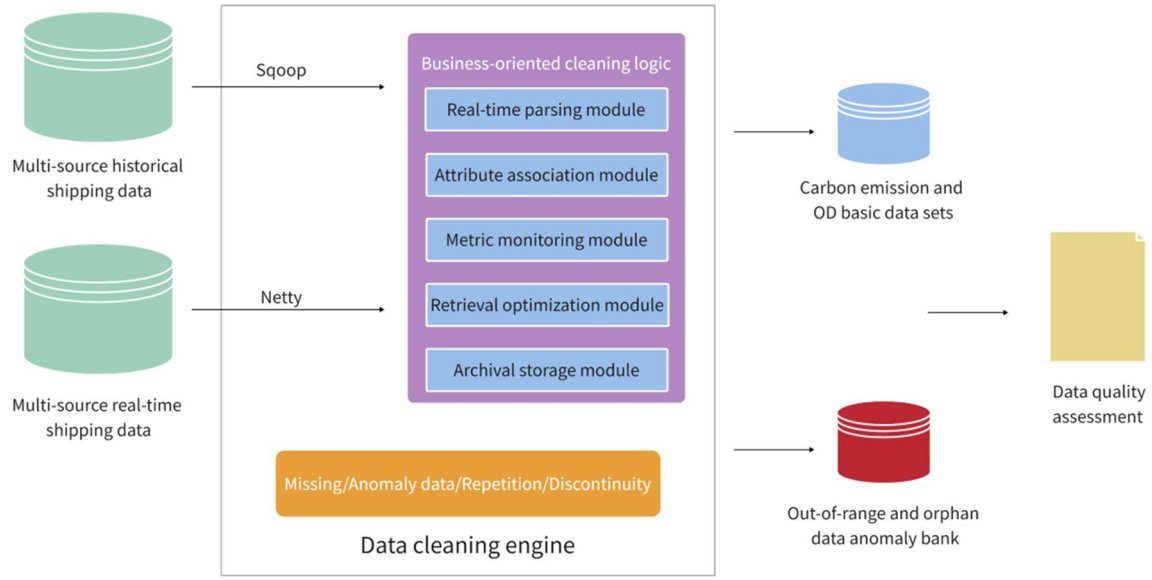

Fig. 2 Schematic diagram of data processing

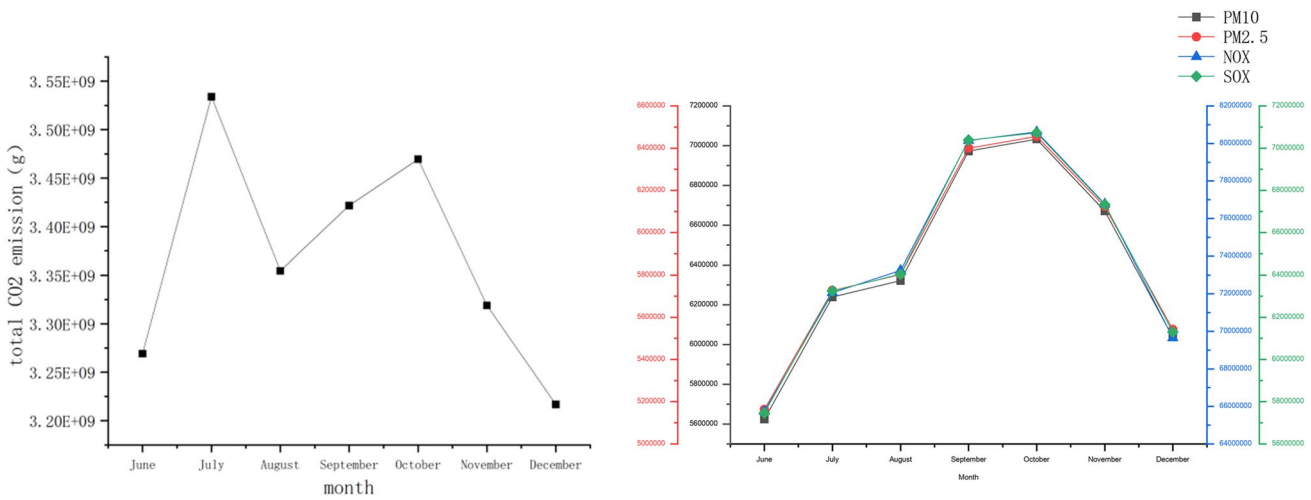

Fig. 3 Total pollutant emissions from ships in the waters near Tianjin Port from June 2018 to December 2018

September. However, due to the influence of the closed fishing season in the Bohai Bay area and sea ice, the carbon emissions of ships in the area near Tianjin Port in June and December are lower than those of other months. The emissions of PM_{10}, $PM_{2.5}$, $NO_{x,}$ and SO_x are also affected by the fishing ban period, with the lowest emissions in June and higher emissions in September, October, and November.

To effectively reduce carbon emissions, relevant departments should strengthen supervision during months with high

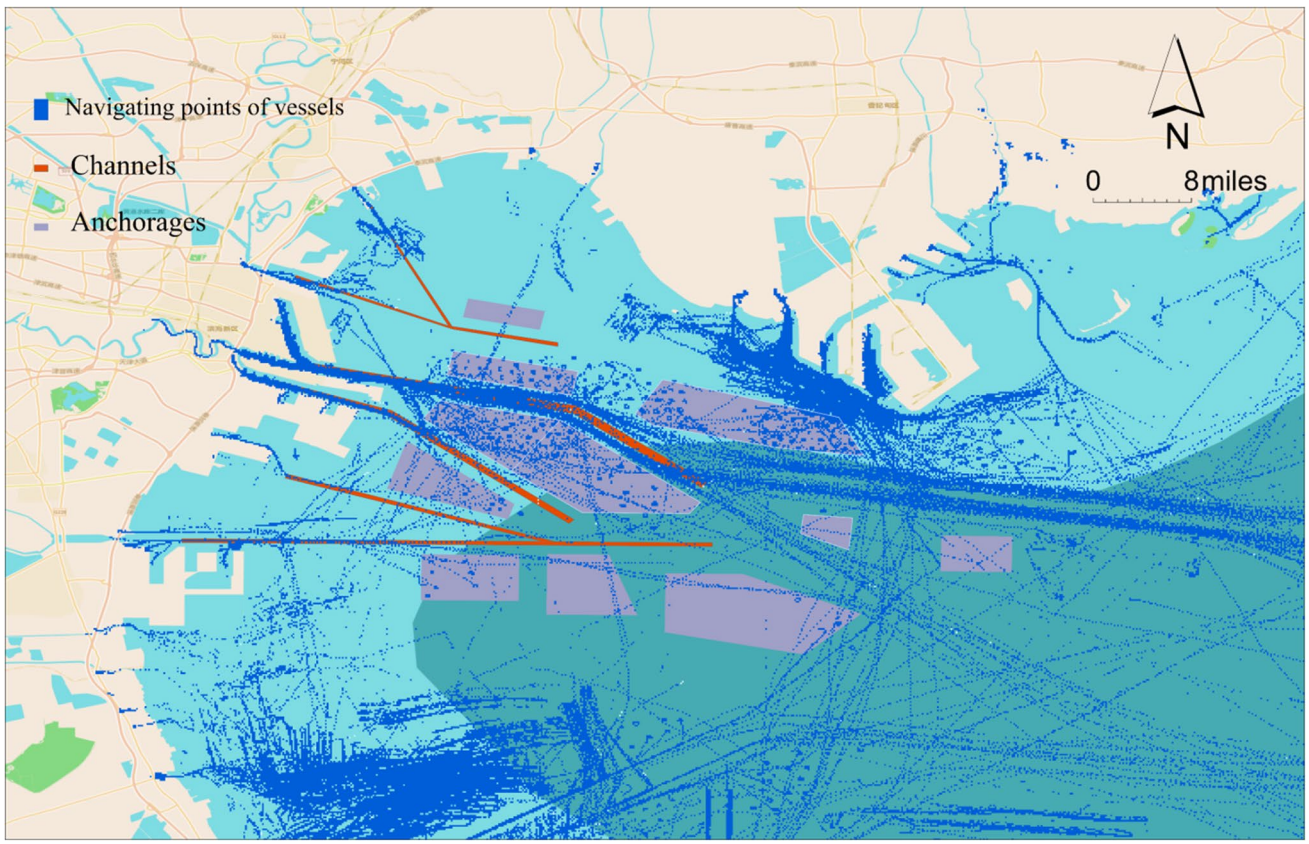

Fig. 4 The spatial distribution of ship carbon emissions in Tianjin Port

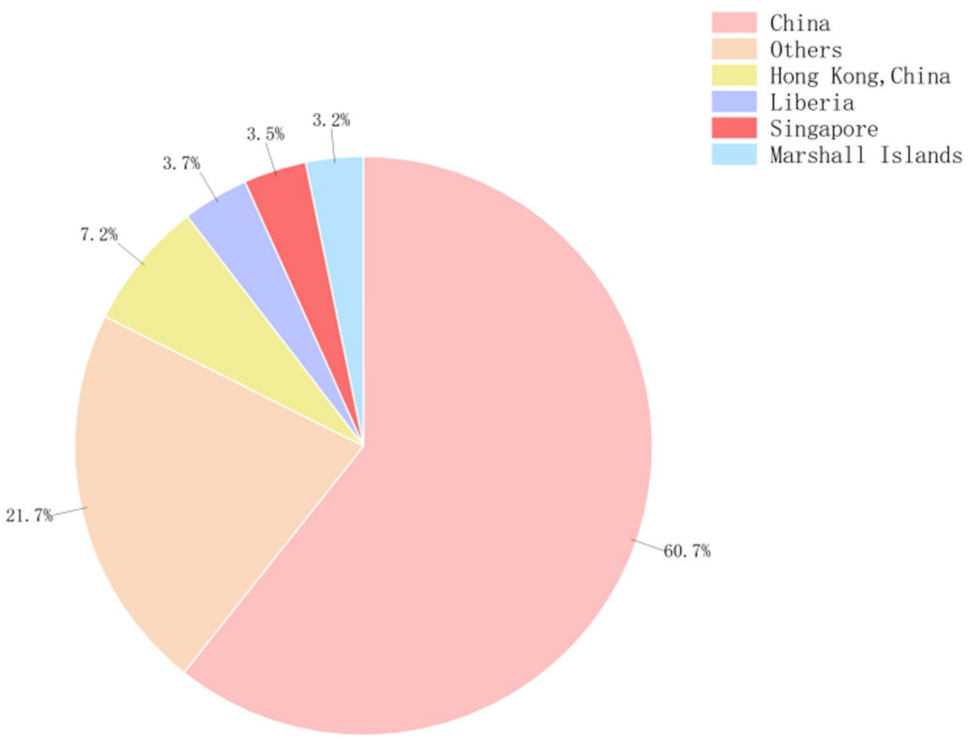

Fig. 5 Carbon emissions from ships of different nationalities

emissions and implement targeted countermeasures based on the specific characteristics of different types of ships.

Ship attribute characteristics: In terms of ship types, carbon emissions of container vessels and dry bulk carriers are relatively higher than other types of ships. In terms of registration place of the ship, China-registered ships emit the most emissions. However, it is also important for regulators to focus on managing emissions from ships registered in other regions, in addition to enforcing emission regulations on Chinese ships.

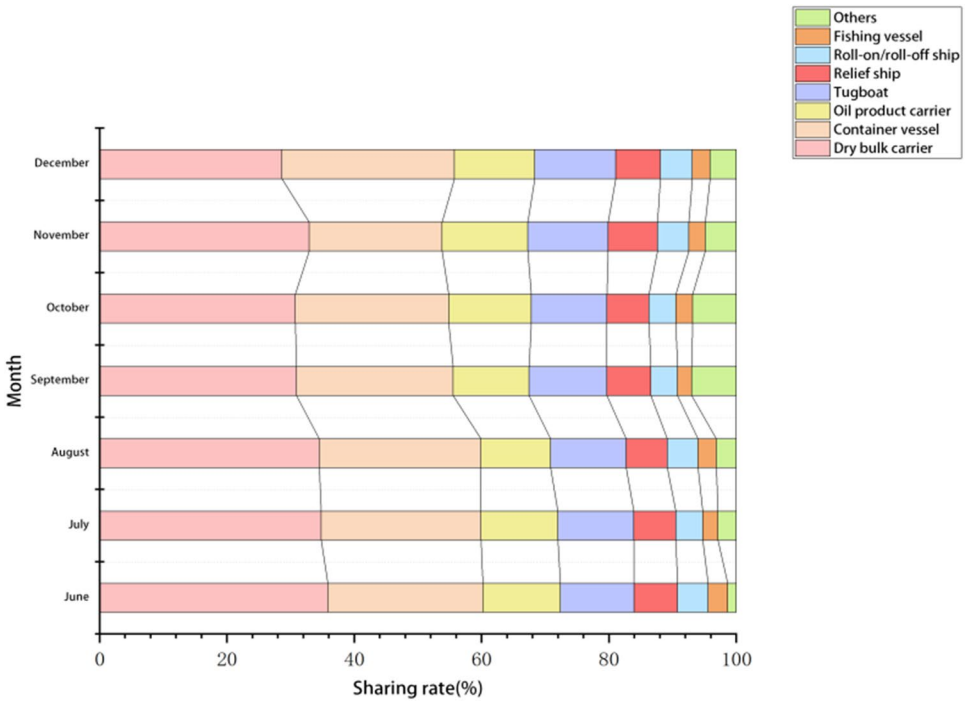

Fig. 6 Pollutant sharing rate of each ship type

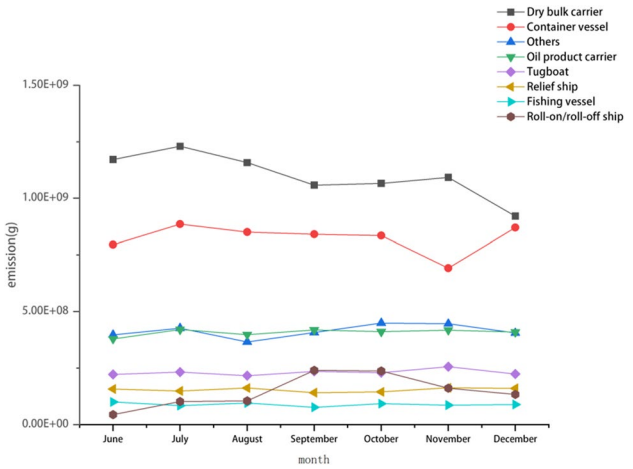

Fig. 7 The distribution of pollutants emitted by different types of ships from June to December in 2018

Ship state characteristics: In terms of ship sailing states, in the low-speed state, carbon emissions of the ship are the most, followed by the cruise state. In the states of berthing and mooring, the amount of carbon emission is the least. However, considering the time of ships in port, the carbon emissions of ships berthing in port are more than those of ships in the maneuvering state (Xu et al., 2021). With the provision of shore power, the carbon emissions from the berthing state are also gradually reduced. Efficient port coordination is necessary to ensure that ships can unload their cargo efficiently and avoid unnecessary waiting time, which can result in additional emissions.

In future work, we plan to further refine the accuracy of carbon emission estimation for port ships in both time and space dimensions. We will also conduct further verification and comparison with other estimation methods to provide more robust data support for relevant regulatory authorities.

Author contribution Peng Wang and Qinyou Hu: designed and performed the experiments, analyzed the data, and prepared the paper.

Wenxin Xie and Lin Wu: participated to collect the materials related to the experiment.

Fei Wang and Qiang Mei: designed the experiments and revised the manuscript.

Funding This research was funded by the National Key Research and Development Program of China, grant number 2018YFC1407400; NSFC No. 61902376; Major Projects of Shanghai Municipal Commission of Science and Technology, No. 18DZ1206300; and Natural Science Foundation of Fujian Province, Nos. 2021J01821 and 2020J05143.

Data availability The data used to support the findings of this study are available from the corresponding author upon request.

Declarations

Ethics approval and consent to participate Not applicable.

Consent for publication Not applicable.

Competing interests The authors declare no conflict of interest.

References

Brodie JE, Lewis SE, Collier CJ, Wooldridge S, Bainbridge ZT, Waterhouse J, Fabricius K (2017) Setting ecologically relevant targets for river pollutant loads to meet marine water quality requirements for the Great Barrier Reef, Australia: a preliminary methodology and analysis. Ocean Coast. Manag. 143:136–147. https://doi.org/10.1016/j.ocecoaman.2016.09.028

Chen D, Zhao Y, Nelson P, Li Y, Wang X, Zhou Y, Guo X (2016) Estimating ship emissions based on AIS data for port of Tianjin. China. Atmos. Environ. 145:10–18. https://doi.org/10.1016/j.atmosenv.2016.08.086

Chen JH, Lu Y (2012) Layout and level division of the development of main ports in the China Bohai Bay. Areal Res. Dev. 31(5):11–15. https://doi.org/10.3969/j.issn.1003-2363.2012.05.003

Chen JH, Xu XM, Meng J, Han LB (2014) Evaluation system and application of port logistics comprehensive service ability in coastal cities. Shanghai Manag. Sci. 36(1):24–30

Endresen Ø, Bakke J, Sørgård E, Berglen TF, Holmvang P (2005) Improved modelling of ship SO2 emissions—a fuel-based approach. Atmos. Environ. 39(20):3621–3628. https://doi.org/10.1016/j.atmosenv.2005.02.041

Endresen Ø, Sørgård E, Behrens HL, Brett PO, Isaksen IS (2007) A historical reconstruction of ships' fuel consumption and emissions. J. Geophys. Res. 112(D12):301–310. https://doi.org/10.1029/2006JD007630

Endresen Ø, Sørgård E, Sundet JK, Dalsøren SB, Isaksen IS, Berglen TF, Gravir G (2003) Emission from international sea transportation and environmental impact. J. Geophys. Res. 108(D17):4560–4570. https://doi.org/10.1029/2002JD002898

European Environment Agency (2019) Annual European Union (EU) LRTAP convention emission inventory report 1990–2017. Publications Office of the European Union, Luxembourg

Government Work Report 2021. The fourth session of the 13th National People's Congress of the People's Republic of China, http://www.gov.cn/guowuyuan/zfgzbg.htm

He LL, Jiao YQ, Jia R, Liang Y (2021) Review on the research status of air pollutant emission in port area: the development of Green Port. J Chongqing Jiaotong Univ. (Nat. Sci.) 40(8):78–87 10.3969-j.issn.1674-0696.2021.08.11

Huang L, Huang HX, Zhou CH, Zhang F, Wen YQ, Xiao CS, Peng X (2019) Spatial-temporal analysis and visualization system for ship exhaust emission in port. J Dalian Maritime Univ. 45(4):146–152. https://doi.org/10.16411/j.cnki.issn1006-7736.2019.04.020

Hulskotte JHJ, Van Der Gon HD (2010) Fuel consumption and associated emissions from seagoing ships at berth derived from an on-board survey. Atmos. Environ. 44(9):1229–1236. https://doi.org/10.1016/j.atmosenv.2009.10.018

International Maritime Organization 1973. International convention for the prevention of pollution from ships,. https://www.imo.org/en/About/Conventions/Pages/International-Convention-for-the-Prevention-of-Pollution-from-Ships-(MARPOL).aspx

International Ship Network 2021. The latest ranking of the world's top ten shipowners, http://www.eworldship.com/html/2021/ship_market_observation_0221/168255.html

Jalkanen JP, Brink A, Kalli J, Pettersson H, Kukkonen J, Stipa T (2009) A modelling system for the exhaust emissions of marine traffic

and its application in the Baltic Sea area. Atmos. Chem. Phys. 9(23):9209–9223. https://doi.org/10.5194/acp-9-9209-2009
Jalkanen JP, Johansson L, Kukkonen (2016) J.A comprehensive inventory of ship traffic exhaust emissions in the European sea areas in 2011. Atmos. Chem. Phys. 16(1):71–84. https://doi.org/10.5194/acp-16-71-2016
Jalkanen JP, Johansson L, Kukkonen J, Brink A, Kalli J, Stipa T (2012) Extension of an assessment model of ship traffic exhaust emissions for particulate matter and carbon monoxide. Atmos. Chem. Phys. 12(5):2641–2659. https://doi.org/10.5194/acp-12-2641-2012
Li MM, Zhou ZJ (2021) Research on ship air pollutant emission list in Gaolan Port of Zhuhai. China Maritime Saf. 2:54–56. https://doi.org/10.16831/j.cnki.issn1673-2278.2021.02.016
Liu B, Zhang W, Han J, Li Y (2021b) Tracing illegal oil discharges from vessels using SAR and AIS in Bohai Sea of China. Ocean Coast. Manag. 211:105783. https://doi.org/10.1016/j.ocecoaman.2021.105783
Liu FW (2009) Ship management, vol 201. Harbin Engineering University Press
Liu J, Wang X, Tan Z, Chen J (2021a) A tripartite evolutionary game analysis of Japan's nuclear wastewater discharge. Ocean Coast. Manag. 214:105896. https://doi.org/10.1016/j.ocecoaman.2021.105896
Liu J, Xie WB, Chen JT (2020) Simulation of emission and diffusion of air pollutants from ships sailing in port. J Xiamen Univ. (Nat. Sci.) 59(6):1016–1024
Liu Y (2018) Study on the vessel emission of ship's atmospheric pollutants based on AIS date in Tianjin Port. Doctoral dissertation, Tianjin Univ. https://doi.org/10.27356/d.cnki.gtjdu.2018.001128
Liu Y, Chen JF, Tian YJ, Wang Z (2021c) Emission characteristics of atmospheric pollutants from ships in sea area around Circum-Bohai Sea Economic Zone. Res. Environ. Sci. 34(3):523–530. https://doi.org/10.13198/j.issn.1001-6929.2020.05.08
Liu Z, Meng Q, Wang S, Sun Z (2014) Global intermodal liner shipping network design. Transportation Research Part E: Logistics and Transportation Review 61:28–39. https://doi.org/10.1016/j.tre.2013.10.006
Lv JH, Fu F, Zuo H, Li SF, He H (2019) Ship emission inventory and its application in Qingdao. Environ. Prot. Sci. 45(5):107–115. https://doi.org/10.16803/j.cnki.issn.1004-6216.2019.05.019
Nandan SN, Rosen S (2009) The commentary of the United Nations convention on the Law of the Sea in 1982. China Ocean Press
Nunes RAO, Alvim-Ferraz MCM, Martins FG, Sousa SIV (2017) The activity-based methodology to assess ship emissions-a review. Environ. Pollut 231(Part 1):87–103. https://doi.org/10.1016/j.envpol.2017.07.099
Peng X, Wen YQ, Xiao CS, Huang L, Zhou CH, Zhang F, Yang TT, Zhang YM (2020) Improved calculation model for ship exhaust emission dispersion. J. Saf. Environ. 20(1):255–264. https://doi.org/10.13637/j.issn.1009-6094.2019.0124
Ren M (2014) EU: start monitoring carbon emissions from large tonnage ships in 2018. (in Chinese). Pearl River Water Transp. 372(23):35. https://doi.org/10.14125/j.cnki.zjsy.2014.23.016
Robinson R (2002) Ports as elements in value-driven chain systems: the new paradigm. Marit. Policy Manag. 29(3):241–255. https://doi.org/10.1080/03088830210132623
Tan Z, Liu H, Shao S, Liu J, Chen J (2021) Efficiency of Chinese ECA policy on the coastal emission with evasion behavior of ships. Ocean Coast. Manag. 208:105635. https://doi.org/10.1016/j.ocecoaman.2021.105635
Tiwari P, Itoh H, Doi M (2003) Shippers' port and carrier selection behaviour in China: a discrete choice analysis. Marit Econ Logist. 5(1):23–39. https://doi.org/10.1057/palgrave.mel.9100062
Wan Z, Ji S, Liu Y, Zhang Q, Chen J, Wang Q (2020) Shipping emission inventories in China's Bohai Bay, Yangtze River Delta, and Pearl River Delta in 2018. Mar. Pollut. Bull. 151:110882. https://doi.org/10.1016/j.marpolbul.2019.110882
Wang J, Huang Z, Liu YY, Chen SY, Wu YC, He YY, Yang XY (2020) Vessels' air pollutant emissions inventory and emission characteristics in the Xiamen emission control area. Environ. Sci. 41(8):3572–3580. https://doi.org/10.13227/j.hjkx.202001067
Wang P, Hu Q, Xu Y, Mei Q, Wang F (2021) Evaluation methods of port dominance: a critical review. Ocean Coast. Manag. 215:105954. https://doi.org/10.1016/j.ocecoaman.2021.105954
Wang ZH, Wang WX, Shi X (2019) AIS data-based ship emission estimation model and real ship verification. J Shanghai Marit. Univ. 40(4):12-16+21. https://doi.org/10.13340/j.jsmu.2019.04.003
Wen YQ, Geng XQ, Huang L, Zhou CH, Liu Y (2017) Calculation model for ship exhaust emissions on a count of the impacts of wind, wave and water current included. J. Saf. Environ. 17(5):1969–1974. https://doi.org/10.13637/j.issn.1009-6094.2017.05.067
Wen YQ, Geng XQ, Wu DY, Zhou CH, Xiao CS, Liu Y, Zheng HT (2015) Measurement model of ship exhaust emissions based on AIS information. Navigation China 38(4):96–101
Wu JH, Wu C, Liu W, Guo JW (2017) Automatic detection and restoration algorithm for trajectory anomalies of ship AIS. Navigation China 40(1):8-12+101
Xu L, Di Z, Chen J, Shi J, Yang C (2021) Evolutionary game analysis on behavior strategies of multiple stakeholders in maritime shore power system. Ocean Coast. Manag. 202:105508. https://doi.org/10.1016/j.ocecoaman.2020.105508
Xu WW, Yin CQ, Xu XJ, Zhang W (2019) Vessel emission inventories and emission characteristics for inland rivers in Jiangsu Province. Environ. Sci. 40(6):2595–2606. https://doi.org/10.13227/j.hjkx.201810207
Ye LF (2015) A study on criminal regulation of marine environmental pollution. Zhejiang:Zhejiang University Press 272
Yuan S, Feng XJ, Zhu YF (2020) Rapid inventory of ship exhaust emissions for inland waterway: a case study in Jiangsu section of Yangtze River. Transp. Res. 6(2):91–100. https://doi.org/10.16503/j.cnki.2095-9931.2020.02.011
Yue H (2018) Global shipping industry adopts strategies for reducing greenhouse gas emissions. Mar. Equip./Mater. Mark. 3:13–14
Zeng FT, Lv J (2020) Ship emission inventory and valuation of eco-efficiency in Xiamen Port. China Environ. Sci. 40(5):2304–2311. https://doi.org/10.19674/j.cnki.issn1000-6923.2020.0264
Zhang J, Lou HJ (2015) Ship management (electronic and electrical major). Shanghai Jiaotong University Press
Zhang JF, Wang WQ, Fang BG, Li MJ (2019) Model for calculating exhaust emissions from ships on Yangtze River. Navigation China 42(2):108–113
Zhang S, Chen J, Wan Z, Yu M, Shu Y, Tan Z, Liu J (2021) Challenges and countermeasures for international ship waste management: IMO, China, United States, and EU. Ocean Coast. Manag. 213:105836. https://doi.org/10.1016/j.ocecoaman.2021.105836
Zhang ZW, Huang ZJ, Xu YQ, Chen WW, Huang L, Bai L, Huang JR, Zhen JY, Yan M (2020) Ship emissions spatial characterization improved method and application based on AIS trajectory restoration. Acta Sci. Circumst. 40(6):1931–1942. https://doi.org/10.13671/j.hjkxxb.2019.0494
Zhu YF, Lei ZY, Feng XJ, Yuan S, Liang WW (2019) River based on AIS big data. Environ. Sci. Tech. 32(4):41–46. https://doi.org/10.3969/j.issn.1674-4829.2019.04.009
Zong G, Hu BB, Han JF (2012) Complexity research on spatial structural characteristics of China's coastal port network. China Soft Science 12:171–178